PAPER

Transient non-classical transport in the hollow cathode plume II: evaluation of models for the anomalous collision frequency

View the article online for updates and enhancements.

Transient non-classical transport in the hollow cathode plume II: evaluation of models for the anomalous collision frequency

Marcel P Georgin[1],[*] and Benjamin A Jorns[2]

[1] University of Michigan, Applied Physics Program, Ann Arbor, Michigan 48109, United States of America
[2] University of Michigan, Department of Aerospace Engineering, Ann Arbor, Michigan 48109, United States of America

E-mail: georginm@umich.edu

CrossMark

Abstract
The ability of fluid-based closure models to describe the non-classical electron collision frequency in the plume of a hollow cathode is experimentally investigated. Six models—all predicated on the assumption that the non-classical collision frequency can be attributed to ion acoustic turbulence (IAT)—are considered. Experimental measurements of the time-resolved plasma properties in the cathode plume (Georgin M P, Jorns B A and Gallimore A D 2020 *Plasma Sources Sci. Technol*, **29** 105010) are used to evaluate each closure model and compare it to experimental measurements of the effective electron collision frequency. Though more than one of the considered closures can predict the time-average behavior of the plasma in the cathode plume, it is found that only one model accurately predicts the measurements in both space and time for the cathode and operating conditions that were studied. This new highest fidelity model is derived using a single-equation approach based on modeling the average frequency of the IAT as it evolves in space and time. The implications of the success of this model are discussed in the context of the understanding of the dynamics of the IAT in the cathode plume as well as on-going fluid-based modeling efforts related to cathode plumes.

Keywords: hollow cathode, plasma waves, plasma turbulence, turbulence modeling, electric propulsion, ion acoustic turbulence, plasma propulsion

(Some figures may appear in colour only in the online journal)

1. Introduction

The thermionic hollow cathode is a low-temperature plasma device that has been widely adopted with applications ranging from fundamental science [1–5] to plasma processing of materials [6, 7]. This system employs a low work-function material [8] in an enclosed geometry [9] to generate a collisional and dense internal plasma that is extracted into a collisionless plume. Although these electron sources have

been extensively deployed in a variety of applications, there remain open questions related to the underlying physical processes, notably in this plume region, that limit our understanding of how these devices operate. For example, under ideal operating conditions, these devices can be designed to stably produce high electron currents (1–1000 A) [8, 10]; however, it has been noted that at the confluence of low flow rate and high current the device transitions to the so-called 'plume mode' where the plasma becomes highly unstable, generating a large, low-frequency ($\sim$100 kHz) oscillation in the discharge

1

current. The amplitude of this oscillation can be >100% of the mean value [11–13]. This transition to instability poses a potential risk for a number of applications—particularly Hall and ion thrusters. Indeed, experimental work by Goebel *et al* [14] coupled with numerical simulations from Mikellides *et al* [15] showed that the presence of this instability is correlated [14] with the production of energetic ions that bombard the cathode's plasma facing surfaces, significantly reducing lifetime [16, 17]. This effect has motivated a number of studies to understand or at least mitigate the transition to plume mode [18, 19]. While this previous body of work has led to several proposed theories to explain the plume mode instability [14, 20, 21], historically, numerical simulations of these devices have not been able to self-consistently predict the transition.

Two recent studies have overcome this limitation, predicting plume mode-like oscillations in fluid-based simulations for the first time [22–24]. The key insight from these investigations was that the inclusion of models for time-resolved non-classical collision frequency allowed for the fluctuations to onset. This innovation was motivated by the results of previous numerical [15, 25] and experimental studies [26, 27] of the cathode plume that showed non-classical collision frequency was necessary to predict the time-averaged electron temperature and plasma potential profiles. Both models for the non-classical collision frequency used in these studies were based on the underlying assumption that this effect can be attributed to the onset of ion acoustic turbulence (IAT) driven by the collisionless process of inverse electron Landau damping. The challenge for a fluid-based model, however, is that this mechanism is an inherently kinetic effect.

To try to represent the non-classical collision frequency in a fluid-based model, it is then necessary to employ approximations, i.e. so-called 'closure models'. Mikellides *et al* [22] implemented an algebraic equation (a 'zero-equation' model) relating the collision frequency to the background, fluid-like plasma properties while Sary *et al* [24, 28] employed a 2D partial differential equation (a 'single-equation' model). Although both codes predict large-scale (0.1–1 cm) and large amplitude plasma oscillations (> 100% peak-to-peak amplitude relative to the mean value) at low flow rate conditions, they have notable spectral differences. The dominant mode in reference [24] is ∼1 MHz, which is ∼20× the typical experimentally observed value. On the other hand, the work in reference [22] found better agreement with direct experiments of the simulated cathode, but still over predicted the oscillation frequency by 3.5× the measured value. These differing implementations led to disparate interpretations about the nature of the oscillation. Mikellides *et al* [22] suggested that the plume mode oscillation is connected to the enhanced Ohmic heating of electrons due to IAT while Sary *et al* [24] concluded that it is the result of periodic saturation of the turbulence. Taken together, although the interpretations differ, these previous studies both provide correlational evidence that non-classical (anomalous) collision frequency (resistivity) is likely a driving factor for the plume mode instability.

The goal of this two part study is to perform a detailed experimental investigation into this time-resolved anomalous
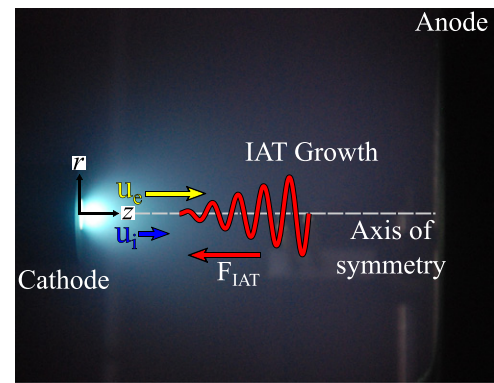
Figure 1. The hollow cathode discharge at 20 A and 5 sccm-Xe. The electrons flow from the cathode to the anode, and experience a drag force due to the growth of IAT in the plume region.

resistivity (or collisionality) in the plasma plume of a hollow cathode. Specifically, we investigate two key tenets of the previous modeling work: that the time-resolved anomalous collision frequency can be attributed to the presence of IAT and that this effect can be represented with a fluid-based closure model. Part I (reference [29]) focused on the first tenet, where we showed experimentally that there are large fluctuations in the effective collision frequency on the time-scale of the plume mode oscillation. We calculated the IAT effect through an application of quasilinear theory informed by direct measurements of the turbulent wave spectrum and showed that this phenomenon is well described by a drag on the electrons induced by IAT. In this work, part II, we proceed under the assumption that the IAT is the driving factor for electron collisionality and focus on validating different fluid closure models for the anomalous collision frequency due to the turbulence.

This paper is organized in the following way. We first introduce in the following section a set of closure models for the anomalous collision frequency for cathode fluid codes. Then, we use our experimental results from [29] (see [29] for experimental details) to evaluate the closure models and compare their predictions to our measurements of the electron collision frequency. We conclude by discussing the implications of the results on our understanding of electron transport in the plume region and hollow cathode modeling.

2. Closure models for the anomalous collision frequency

Figure 1 shows the canonical geometry for a hollow cathode discharge and the process by which the growth of IAT can lead to an effective collision frequency. Electrons transit from the cathode to the anode with drift $\vec{u}_e$. This drift gives rise to the growth of a turbulent spectrum of ion acoustic waves through inverse electron Landau damping. Energy is thus extracted from the electron flow in a process that can be represented as an effective drag force on this species, $\vec{F}_{IAT} = -m_e \nu_{an}^{IAT} \vec{u}_e$ where m_e is the electron mass and ν_{an}^{IAT} denotes an effective collision frequency. From quasilinear theory [30], we can express the collision frequency in terms of a sum over the spectrum of

electrostatic modes associated with the IAT:

$$\nu_{\mathrm{an}}^{\mathrm{IAT}} = \sqrt{\frac{\pi}{2}\frac{m_{\mathrm{i}}}{m_{\mathrm{e}}}}\frac{1}{n_{\mathrm{e}}T_{\mathrm{e}}}\sum_k \omega_k W_k \ , \tag{1}$$

where m_{i} is the ion mass, n_{e} is the electron density, and ω_k and W_k are the frequency and energy density, respectively, of a mode with wavevector, k. Following definitions for ion acoustic modes from part I, we know that $W_k/n_{\mathrm{e}}T_{\mathrm{e}} \equiv (\tilde{\phi}_k/T_{\mathrm{e}})^2$. Here, $\tilde{\phi}_k$ is a potential fluctuation, n_{e} is the electron density, and T_{e} is the electron temperature. These latter two parameters vary relatively slowly in time on the plume mode time-scale. In part I, we showed using time-resolved measurements of the IAT spectrum that this expression yields values quantitatively and qualitatively consistent with the measured oscillation in electron collision frequency. Moreover, this non-classical IAT effect is orders of magnitude higher than contributions from classical collisions.

While we had experimental measurements of the IAT properties necessary to evaluate (1) in part I, the challenge with implementing this in a fluid code is that the onset and growth of the ion acoustic waves and their interaction with the electrons are inherently kinetic effects. Since these processes cannot be captured self-consistently in a fluid framework, such models must employ fluid-like approximations for the wave properties. As we noted earlier, there are multiple approaches that have been employed to achieve this end. In the following sections, we first review the quasilinear approximation of the anomalous collision frequency and how to express this in terms of macroscopic wave properties, like the average frequency and total wave energy density. Then we discuss the zero- and single-equation closure models that build upon these initial approximations.

We remark that all of the methods to date for closures in the cathode plume can be understood with respect to a common framework. In particular, we can define a frequency averaged over the IAT spectrum as $\langle\omega\rangle$ by approximating the sum in equation (1) with an integral such that $\langle\omega\rangle = \int \omega_k W_k \mathrm{d}k/\int W_k \mathrm{d}k$. We further can define the total wave energy density as $W = \int W_k \mathrm{d}k$. Subject to these two definitions, we can re-cast equation (1) as

$$\nu_{\mathrm{an}} = \langle\omega\rangle\sqrt{\frac{\pi}{2}\frac{m_{\mathrm{i}}}{m_{\mathrm{e}}}\frac{W}{n_{\mathrm{e}}T_{\mathrm{e}}}}. \tag{2}$$

This translates the issue of closure in fluid simulations for the cathode to a problem of finding expressions for the average frequency and wave energy density as functions of the background, fluid-like properties of the plasma (e.g. n_{e}, T_{e}, u_{e}, etc). Closure models to date for hollow cathode plumes have either been zero- or single-equation based. In the zero-equation case, analytical expressions are assumed for both the average frequency and wave energy density [25]. In the single-equation case, an analytical expression for the average wave frequency is used, and a PDE for the evolution of the total wave energy density is solved [23, 28]. In the following discussion, we review the results from different approaches that have been applied to date. We also derive a new, single-equation closure

model based on tracking the evolution of the average frequency of the distribution.

2.1. Zero-equation closures

Cathode simulations that employ a zero-equation closure use physically-informed assumptions about the plasma and IAT state to find algebraic expressions for the wave energy density and average frequency as they depend on typical fluid plasma parameters. This is the approach applied by Mikellides *et al* in the Orca2D code [25] where they adopted the Sagdeev closure model [30]. In this case, the shape and magnitude of the IAT spectrum is assumed to result from the balance of nonlinear ion Landau damping with linear growth from electron inverse Landau damping at steady state. This leads to an expression for the total wave energy density:

$$W \simeq \beta M_{\mathrm{e}}\frac{T_{\mathrm{e}}}{T_{\mathrm{i}}}n_{\mathrm{e}}T_{\mathrm{e}} \ , \tag{3}$$

where β is a constant [30] and T_{i} is the ion temperature. In this expression, the dependence on the electron Mach number stems from the linear growth of the waves while the ratio $T_{\mathrm{e}}/T_{\mathrm{i}}$ is from nonlinear ion Landau damping that can dominate as the amplitude of the oscillations increases. We combine this approximation with the physically plausible assumption that the average frequency scales with the ion plasma frequency, i.e. $\langle\omega\rangle \sim \epsilon\omega_{\mathrm{pi}}$, where ϵ is a constant of proportionality. Combining these results with equation (2), we find that the anomalous collision frequency reduces to

$$\nu_{\mathrm{an}}^{\mathrm{SG}} = \alpha_{\mathrm{sat}}M_{\mathrm{e}}\frac{T_{\mathrm{e}}}{T_{\mathrm{i}}}\omega_{\mathrm{pe}}, \tag{4}$$

where $\alpha_{\mathrm{sat}} \equiv \beta\epsilon$ is now a modified constant of proportionality that is known to be of order 0.01 [31]. Using this relation, Mikellides *et al* [25] were able to successfully predict the plasma potential profile in the NSTAR hollow cathode. More recently, we note that these authors also have found quantitative agreement between their simulations and global measurements of the cathode plume mode oscillation [22]. In this latter work, the authors did not specify α_{sat}, *a priori*, but rather iterated upon it until they were able to match experimental measurements of the discharge current in the simulated cathode. It was remarked upon in this previous work that this numerically identified coefficient was within a factor of two of the theoretical value of $\alpha_{\mathrm{sat}} = 0.01$.

Lastly, evaluating (4) requires that we employ an additional assumption on the ion temperature, a quantity we could not measure in our experimental configuration. In this model, and in closures we evaluate later, we assume that the ion temperature is constant in time and that its magnitude is $\sim 0.1\langle T_{\mathrm{e}}\rangle$, where $\langle T_{\mathrm{e}}\rangle$ is the time average electron temperature. This assumption is commonly applied in the analysis of plasmas used for propulsion [32] and has been suggested by numerical simulations [22] of similar cathode configurations. Note, however, that there are differences in anode location and geometry with our configuration and that they have applied a magnetic field. We discuss the implications of this assumption in greater detail in section 5.1.

We note here that there are other zero-equation closure models that have been proposed for kinetic, streaming instabilities in other applications [33] that have not been applied to hollow cathode simulations. These models still assume the average frequency scales with the ion plasma frequency. For the wave energy density, on the other hand, we may simply assume that the total energy cannot exceed the thermal energy density i.e. $W = \beta n_e T_e$ or the electron kinetic energy: $W = \beta n_e m_e u_e^2$. These two limits yield the closures:

$$\nu_{an}^{TE} \simeq \alpha_{sat}\omega_{pe}, \qquad (5)$$

$$\nu_{an}^{KE} \simeq \alpha_{sat}M_e^2\omega_{pe}. \qquad (6)$$

These saturation models for the collision frequency have not been applied in cathode simulations to date, but we include them here for comparison.

2.2. Single-equation closure: wave energy density

Even though saturated models for the IAT anomalous collision frequency provide a relatively simple way to estimate the effects of the turbulence on the electrons, it has limitations in fidelity. For example, earlier experimental measurements indicated that the IAT grows spatially [27] in the plume according to a quasilinear wave energy equation. To try to capture this type of wave growth numerically, more recent approaches such as those in [23, 28] employ a single-equation closure where a linear wave energy equation for the IAT wave energy density is solved. This approximation for the growth of IAT, however, neglects nonlinear phenomena—such as those accounted for by the Sagdeev model—that may be occurring the plasma.

The governing structure for this equation is based on following the energy density of one wavepacket in the spectrum with wavevector k such that [34]

$$\frac{\partial W_k}{\partial t} + \nabla \cdot (\vec{v}_{g(k)}W_k) = 2\gamma_k W_k . \qquad (7)$$

Here γ_k is the linear growth rate of an ion acoustic mode with wavevector k and $v_{g(k)} = \partial \omega/\partial k$ is the wave group velocity. To relate this to the total wave energy, W, of the IAT spectrum which is comprised of multiple concurrently propagating wave packets, we integrate (7) over wavevector:

$$\frac{\partial W}{\partial t} + \nabla \cdot (\langle \vec{v}_g \rangle W) = 2\langle \gamma \rangle W, \qquad (8)$$

where $\langle .. \rangle = \int [..]W_k \mathrm{d}k/W$ denotes spectrum averaged quantities. Physically, the two terms on the left-hand-side represent the convection of average IAT wave energy while the contributions to the right-hand-side of (8) represent its sources and sinks from the linear growth rate. We provide an additional discussion about the validity of neglecting nonlinear effects in our plasma in section 5.1. Combining (2) with (8), the anomalous collision frequency can be calculated in space and time. However, the equations are not closed as we require either a measurement or an assumption on the shape of the IAT spectrum in frequency space to estimate the spectrum averaged quantities such as the growth rate and group velocity.

Different numerical models employ distinct approximations of the IAT spectrum to close the governing equations for the wave energy density and collision frequencies. Sary *et al* [23], for example, assume that the energy is concentrated at the frequency that corresponds to the fastest growth rate. Although they do not adopt the formalism of average wave spectrum properties that we have introduced here, this approach can be represented equivalently in our framework by making the assumption that the power spectrum is characterized by a delta function in frequency space that corresponds to the frequency of maximum growth. This yields [23]

$$\langle \gamma \rangle = \frac{\sqrt{\pi}}{9}\omega_{pi}\left[\left(\sqrt{\frac{3}{2}}M_e - \sqrt{\frac{m_e}{m_i}}\right) - \left(\frac{T_e}{T_i}\right)^{\frac{3}{2}} e^{-\frac{T_e}{3T_i}}\right]$$
$$- \frac{\nu_{in}}{2}. \qquad (9)$$

Here, ν_{in} is the ion-neutral collision frequency. The governing equations are completed by assuming the average frequency of the spectrum scales with the ion plasma frequency $\langle \omega \rangle \approx \omega_{pi}$. We note that using this approach, Sary *et al* were able to show predicted oscillations with wavelengths that are qualitatively consistent with experimental measurements of the plume mode instability that have been reported in other experimental studies [19]. However, the magnitude of the predicted potential oscillations exceeded the on-axis measurement by a factor of two, and the frequency of the dominant mode exceeded typical values [14] by at least a factor of 10.

As an alternative, Lopez-Ortega *et al* [28] assumed a power-law frequency dependence for the IAT amplitude in the spectrum. This yielded an effective average growth rate of

$$\langle \gamma \rangle = \omega_0 \left[\sqrt{\frac{\pi}{2}}\left(M_e - \left(\frac{T_e}{T_i}\right)^{\frac{3}{2}} e^{-\frac{T_e}{2T_i}}\right) - \frac{\nu_{in}}{2\omega_0}\right], \qquad (10)$$

where ω_0 is the lower-bound cutoff frequency for the IAT spectrum, which is a assumed to be a constant in space and time. Although these authors also did not adopt the formalism we show in (2), as with Sary *et al*, their approach effectively can be interpreted as assuming that the average frequency of the spectrum still scales with the ion plasma frequency $\langle \omega \rangle \propto \omega_{pi}$. Armed with this assumption and using (10), Lopez-Ortega *et al* treated ω_0 as a free parameter and varied it until they were able to show a high degree of time-average agreement in plasma properties with experimental values [28].

2.3. Single-equation closure: average wave frequency

Sary *et al* and Lopez-Ortega *et al* effectively both assumed an algebraic expression for the average collision frequency and solved a differential equation for the IAT wave energy density. To be comprehensive in evaluating single-equation closures, the natural complement is to consider an alternative based on assuming an algebraic expression for the wave energy density and instead tracking the average frequency. This formulation, however, has yet to be made for the cathode plasma.

We derive here a new closure model for the IAT average frequency to address this gap. Our approach follows loosely the work outlined by Lafleur in examining the effects of turbulence
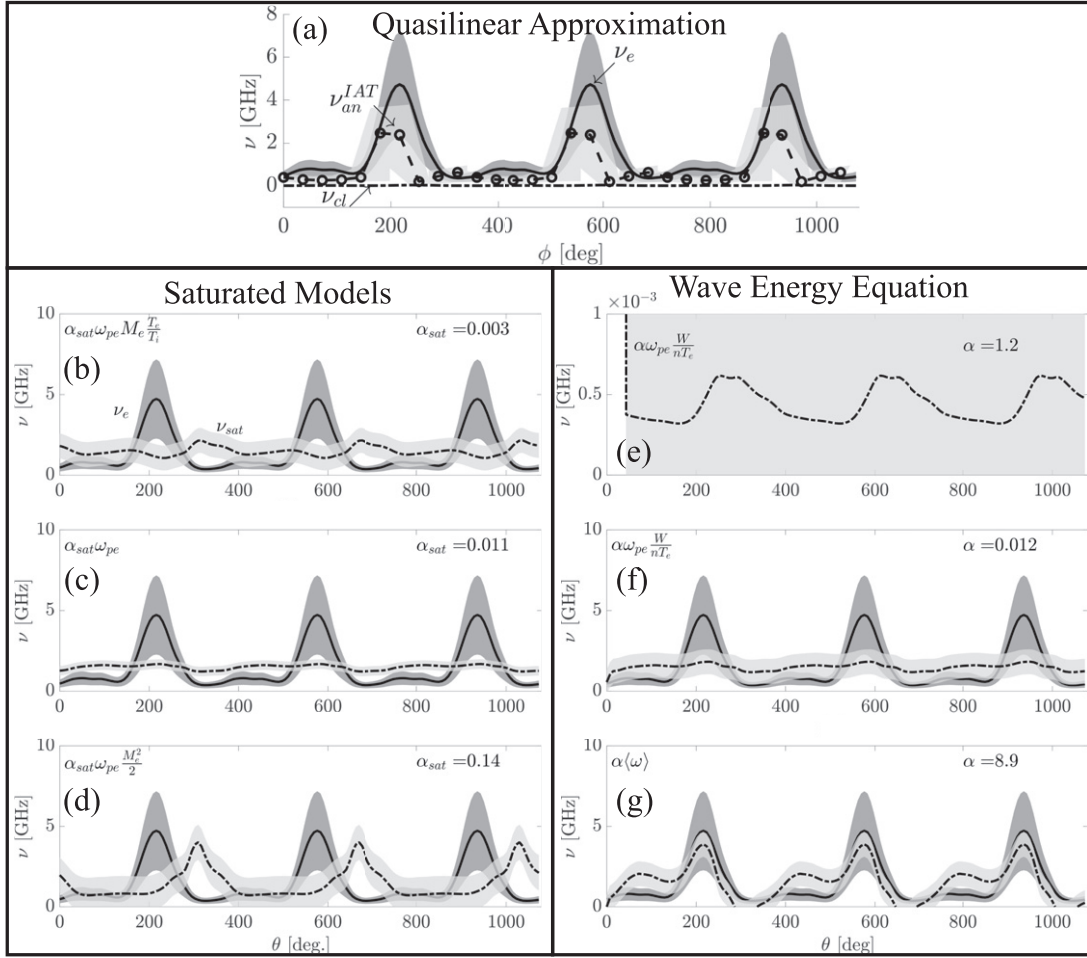
Figure 2. Comparison of the measured collision frequency and the implemented closure models as a function of phase angle. (a) shows the measured collision frequency and contribution from IAT according to the quasilinear approximation in (1). Zero-equation closure models based on assuming wave energy density is saturated in the Sagdeev limit in (b), the thermal energy limit in (c) and the kinetic energy limit in (d). Single-equation closure models based on solving wave energy equation with (9) as the growth rate in (e) and with (10) as the growth rate in (f). (g) shows single equation closure based on solving the average frequency equation using (13). The value of α in each figure is set by equating the time average value of the model to the measured collision frequency at $z = 0.5$ cm. The oscillation frequency is $f = 40$ kHz.

for Hall thrusters [35]. First, we make the assumption that the IAT wave energy saturates to the thermal limit, i.e. $W = n_e T_e$. This assumption is physically tied to the notion that the energy density of the waves cannot exceed that of the plasma. The quasilinear expression for the anomalous collision frequency in (2) thus can be expressed solely as a function of the average spectrum frequency:

$$\nu_{an}^{IAT} = \sqrt{\frac{\pi}{2}\frac{m_i}{m_e}}\langle\omega\rangle. \tag{11}$$

To find an expression for this average frequency, we first revisit the term $\langle\gamma\rangle$ in (8), which can be written under the assumption that the ion drift and ion sound speed are negligible compared to the electron drift as [27, 34]

$$\langle\gamma\rangle = \langle kc_s\rangle\sqrt{\frac{\pi}{2}}\left(M_e - \left(\frac{T_e}{T_i}\right)^{\frac{3}{2}}e^{-\frac{T_e}{2T_i}}\right) - \frac{1}{2}\nu_{in} \tag{12}$$

From the dispersion relation for acoustic modes in the limit of small wavenumber, we have $\langle kc_s\rangle = \langle\omega_r\rangle/(1 + M_i)$, where we

have introduced the ion Mach number ($M_i = u_i/c_s$). Given that the electron Mach number is relatively constant in the plume (see figure 2 in part I) the ion Mach number likely follows a similar trend. Thus, we make the further simplification that this Mach number is approximately constant in the region of interest such that within a constant of proportionality, α, we find $\langle kc_s\rangle \approx \langle\omega\rangle/\alpha$.

We use this result in (12) and combine with (8) in the limit $W = n_e T_e$ to solve for the average spectrum frequency:

$$\langle\omega\rangle = \alpha\left(\frac{\frac{\partial n_e T_e}{\partial t} + \nabla\cdot(n_e T_e\langle v_g\rangle) + n_e T_e\nu_{in}}{n_e T_e\sqrt{2\pi}\left(M_e - \left(\frac{T_e}{T_i}\right)^{3/2}e^{-T_e/2T_i}\right)}\right) \tag{13}$$

This result captures the physical process that the energy in the IAT spectrum will be shifted to different frequencies/wavelengths, as the spectrum propagates in the plasma. Indeed, this change in average frequency is necessary to satisfy the wave energy equation when the total energy is assumed to have saturated thermally. Physically, (13) indicates that the

average frequency is primarily tied to two processes: the rate of IAT wave energy convection and ion-neutral collisions. In particular, the scaling with ν_{in} (which is typically $\mathcal{O}$ (1 MHz)) effectively introduces a minimum average spectral frequency. This expectation for the IAT average frequency agrees with earlier experimental results [19, 27, 29] that show the IAT average frequency is well below ω_{pi}, the commonly used scaling parameter for the average frequency. This model, along with equation (11), thus yields the final expression that we analyze to estimate the anomalous collision frequency.

3. Methods for evaluating closures with experimental data

In the following discussion, our goal is to use the experimental data we collected in part I to compare the measured electron collision frequency to predictions from the closure models presented above. For the zero-equation closures (see section 2.1) and the single-equation closure based on wave frequency (see section 2.3), we can simply substitute the measured background plasma properties and gradients in the governing equations. For the single-equation closures that depend on the evolution of the wave energy density (see section 2.2), however, we must numerically solve for this quantity through (8) using experimental data for the coefficients in the PDE. To this end, in the following analysis, our results for these closures stem from discretizing this expression as

$$W_{(m,n+1)} = W_{(m,n)}(1 + \Delta t \gamma_{m,n}) - \Delta t \nabla_x W_{(m,n)}$$
$$\nabla_x W_{(m,n)} = \frac{c_{s(m+1,n)} W_{(m+1,n)} - c_{s(m,n)} W_{(m,n)}}{\Delta x} , \quad (14)$$

where $n \in 0, 1, 2, \ldots$ and indicates the time index and $m \in 0, 1, 2, \ldots, M$ represents the spatial index for $M + 1$ discrete locations where measurements were performed. The time step, $\Delta t = 0.556\ \mu$s is determined by the time resolution of the measurement of the plasma parameters, and the spatial step is $\Delta x = 0.1$ cm. We use the measured wave energy density as an initial condition for the PDE, and we assume at the downstream location of the measurement domain that the spatial derivative at the Mth location is equal to the spatial derivative at the $M + 1$ location. Following the previous work of [24], we bound the solution for the IAT wave energy with the thermal energy density of the plasma to prevent unbounded solutions: $10^{-5} < W < nqT_e$.

4. Results

In this section, we compare the measured electron collision frequency to the estimates of the anomalous collision frequency provided by the above closure models. We first examine the result at a single point in the middle of the domain to quantitatively examine the fidelity of these approximations. Then we investigate trends in our findings in time over the whole measurement region.

4.1. Single point comparisons of the anomalous collision frequency models

In this section, we evaluate the closures presented in equations (2)–(13) with experimental data at the same downstream location we examined in part I, $z = 0.5$ cm from the cathode exit. The results in figure 2 are plotted as a function of phase angle with respect to a reference signal, the oscillation in the discharge current when the cathode is in plume mode. This choice is tied to the time-resolved, phase-averaging approach we presented in part I. In order to increase the signal to noise for our measurements, we used the discharge current as a trigger point to average over multiple cycles of the plume mode. Before averaging these cycles, it was necessary to compensate for the small but natural variations in the plume mode oscillation frequency, which has a mean value of $f = 40$ kHz, by converting each cycle into relative phase with respect to the discharge current. On average, there is an approximate relationship between the plotted phase, θ, and time, t, given by $t = \theta/360/f$. In each plot in figure 2, we show the measured electron collision frequency (solid line) as well as the results from the closure models (dashed line). The gray bands in these figures represent the statistical uncertainty in the measurement techniques (described in part I).

As an initial point of reference, we briefly summarize the major finding from part I graphically in figure 2(a). This shows a comparison among the measured collision frequency, the anomalous collision frequency from (1), and the classical collision frequency, ν_{cl}. We evaluated the anomalous contribution using measurements of the wave energy density and the classical component using the standard forms for Coulomb [36] and neutral collision frequencies [32]. As was noted in part I, the marked agreement between the quasilinear approximation (see equation (1)) and the measured electron collision frequency indicates that changes in the IAT properties are the dominant contributor to the variations in electron collision frequency. This is direct experimental evidence that lends support to the approach of using models for the IAT to derive closures for the electron collision frequency. Figures 2(b)–(g) show the results of these closure models explicitly, which we discuss in the following.

4.1.1. Zero-equation closures. We first consider the three saturated anomalous collision frequency models. In each of these cases, we have adjusted the parameter α such that the time-average value of the IAT collision frequency is equal to the time-average of the measured electron collision frequency at $z = 0.5$ cm. The value of α for each model, determined from the data, is indicated in the top right corner of each subfigure of figure 2.

Figure 2(b) shows the closure model for ν_{sat} derived under the assumption the wave energy density is saturated in the Sagdeev limit (equation (3)). Both qualitatively and quantitatively, this model does not capture both the time-resolved behavior of the measured collision frequency. The closure expression distinctly lags the actual electron frequency in phase ($\sim 90°$), and the mean amplitude of the oscillation is smaller by a factor of two. This result is perhaps surprising, given the success of the numerical model in reference [22].

Our finding may point to ion temperature fluctuations, which we have not considered here, playing a more important role in the plume mode oscillation than previously believed. This further motivates future studies of evolution of the ion temperature and its connection to wave-driven heating on these time-scales, which could improve the agreement of this closure with experiments as was noted in reference [22]. We provide an additional discussion on this topic further in section 5.1.

Figure 2(c) shows the measured collision frequency and the closure model for anomalous collision frequency derived assuming the IAT saturates in the thermal limit (equation (5)). As with the Sagdeev closure model, we see there is poor agreement with the measurement. The shape of the waveform for this closure is inverted compared to the measured collision frequency, and the amplitude of the oscillation is an order of magnitude smaller.

In figure 2(d), we show the closure model for collision frequency derived by assuming the waves are saturated in the kinetic energy limit (equation (6)). The amplitude of the collision frequency oscillation is comparable to the amplitude exhibited by the measured collision frequency. However, it has a characteristic phase lag similar to the lag exhibited by the Sagdeev model.

Although none of these zero-equation closures accurately captures the measured collision frequency, we do note that in comparing the results from figures 2(b) and (c), the two closures that depend on the electron Mach number (equivalently electron drift) appear to show qualitative features similar with the measured result. Physically, this connection is likely related to the fact that the growth of IAT is driven by and thus correlated with the electron drift (see equation (10)). With that said, the general lack of agreement calls into question the key simplifying assumptions of these closures: that the IAT wave energy density is saturated and the average frequency of the spectrum is proportional to the ion plasma frequency. In search of more accurate methods for approximating the evolution of the anomalous collision frequency in time, we explore in the next section the results of the closure models that relax the first of these assumptions.

4.1.2. Single-equation closures.　We explore in this section the closure models for the collision frequency derived by first assuming the average frequency of the IAT scales with the ion plasma frequency and then solving (8) for the evolution of the average wave energy. Figure 2(e) shows the result for the model predicated on the assumption that the average growth of the wave energy scales with the plasma frequency as indicated by (9). We have reduced the scale in this plot by four orders of magnitude compared to the other sub-figures in order to illustrate the features. Although the predicted collision frequency exhibits oscillations similar to, if not in phase with, the measured value, the amplitude of variation in the collision frequency is several orders of magnitude too small. This is the result of immediate damping of the solution for wave energy density down to the imposed constant lower bound. We observe variation in the collision frequency, however, because it is proportional to the plasma frequency, which varies in time.

Figure 2(f) shows the IAT collision frequency determined from the single-equation closure model where the average growth rate is assumed to be an adjustable constant. In this case, we have elected to use $\omega_0 \sim 2\pi\nu_{\text{in}}$, where ν_{in} is the local time-averaged ion-neutral collision frequency. This choice is consistent in magnitude with observations from previous experimental measurements [27]. We immediately note that this result is almost identical to the result shown in 2(c). This stems from the fact that the predicted wave growth is very rapid compared to the time-scale of the plume mode oscillation, saturating almost immediately to our imposed upperbound of $W = nT_e$. This leads to the same calculated value of α_{sat} as in the simple zero-equation closure model assuming the waves *a priori* saturate to the thermal upperbound.

In both cases, figures 2(d) and (e), we thus find that the single-equation models that assume an average frequency and solve for the IAT wave energy density tend to grow to saturation and then oscillate at the imposed bounds. Although this leads to estimates for the collision frequency that are not consistent with experimental measurements, this process does suggest the possibility that it may be physically reasonable for the wave energy to saturate on the time-scale of the oscillations. If this is the case, then the variation in collision frequency would stem not from the oscillations in average wave energy but rather the average frequency at which this spectrum exchanges energy with the electrons, $\langle\omega\rangle$. This motivates the last closure model we derived in section 2.3.

We show the results of this final closure model in figure 2(g) where we have coupled the assumption of thermally saturated IAT with an expression for the average IAT frequency as given by (13). Here, we find that the measured and calculated waveforms are highly correlated and agree within the statistical uncertainty shown by the gray bands. The relative success of this model, in comparison to the other closure attempts, seems to support the hypothesis that the wave energy is saturated while the variation in collision frequency stems from the fluctuations in the average IAT frequency. We expand on this interpretation with greater detail in section 5.2.

To summarize, the results in figures 2(a)–(g) show that most of the models implemented in hollow cathode simulations to date have limited fidelity with regards to capturing the transient characteristics of the electron collision frequency. Only one of the zero-equation closures exhibits comparable wave amplitude (kinetic energy limit), and the single-equation closures for the IAT wave energy density all tend to saturate at the bounds we imposed. Only the novel single-equation closure model that we presented for the first time in this work yields an approximation with quantitative agreement to the measured value.

4.2. Qualitative 1D comparisons of the anomalous collision frequency models to the electron collision frequency

This section expands the preceding single-point results to a spatial comparison of closure models along the axis of the cathode centerline. To this end, we first recall in figures 3(a) and (b) the key results from part I. Here we show the measured electron collision frequency in figure 3(a) and the contribution to collision frequency from the IAT calculated with
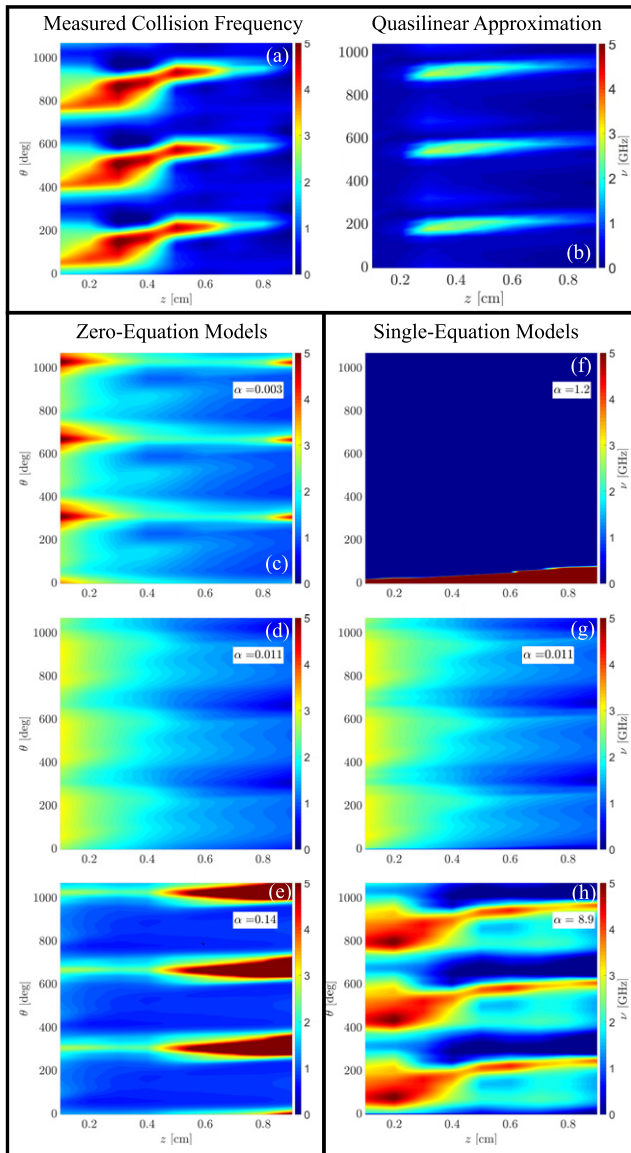
Figure 3. Comparison of the measured collision frequency and the implemented closure models for the IAT as a function of position and phase angle. (a) shows the measured collision frequency. (b) shows the quasilinear approximation using (1). The zero-equation closure models based on assuming the wave energy density is saturated in the Sagdeev (c), thermal (d), and kinetic energy (e) limits. Single equation closure models based on solving the wave energy equation with (9) as the growth rate in (f) and with (10) as the growth rate in (g). (h) shows the single-equation closure based on solving the average frequency using (13). The value of α is set by equating the time average value of the model to the measured collision frequency at $z = 0.5$ cm. The oscillation frequency is $f = 40$ kHz.

the quasilinear formulation (see equation (1)) in figure 3(b). As we discussed in part I, the IAT-driven collision frequency agrees qualitatively and quantitatively (to within experimental uncertainty) with the measured value between $z = 0.3$ cm and 0.9 cm. This critical finding suggests that we can approximate the measured electron collision frequency with the anomalous collision frequency due to IAT for the majority of the measured plume region. We do note that closer to the cathode,

however, there is disagreement between measurement and the IAT contribution to the collision frequency. We speculated in part I this could be attributed to perturbations in the IAT waves induced by the presence of the plasma probes. With that said, aside from these upstream points, the overall agreement validates the use of closure models for the collision frequency that are predicated on modeling the effects of the IAT. We contrast in the following the results of these closure models with the measured collision frequency along the cathode axis over time.

We show in figures 3(c)–(e) the zero-equation results for the dependence of collision frequency along the axis of the discharge and as a function of phase angle with respect to the a current oscillation. Respectively, these are the models that assume wave saturation based on the Sagdeev, thermal, and kinetic energy limits. We find that all of these approximations mirror the results from the single-point comparisons shown in figures 2(b)–(d). The oscillations in predicted collision frequency lag the measured value in phase and do not match in amplitude.

Figures 3(f)–(g) plot the single-equation closure models for the collision frequency. Respectively, these figures are based on the models proposed by Sary *et al* [24] (see (9)), Lopez-Ortega *et al* [28] (see (10)), and the new closure we have derived (see (13)). Following the trends identified in figures 2(e)–(g), we find that the model employed by Sary *et al* quickly damps, the Lopez-Ortega model saturates to the thermal limit (see figure 3(d) for comparison) and that our model for the IAT average frequency shows the best quantitative agreement with the measured value.

In a direct parallel to our earlier findings in figure 2, the success of this closure over the whole experimental domain further lends credence to our hypothesis that the IAT wave energy can be treated as saturated on this time-scale and that the variations in collision frequency are driven by changes in the average IAT frequency. Interestingly, we note that this expression for closure produces results that yield a better match to experiment than the contribution for IAT collision frequency calculated from direct measurements of the IAT properties in figure 3(b). This favorable comparison may ultimately be a consequence of the fact that the wave probe measurements become less reliable as they approach the cathode, whereas we have greater confidence in the background properties that inform the closure model. We expand on this explanation as well as the physical significance of the success of this modeling in the following section.

5. Discussion

The experimental measurements from part I [29] and the above analysis of closure models highlight the challenges for capturing the inherently kinetic effects of IAT-driven collision frequency in a fluid-based framework. In particular, we have found that the previously employed closures do not appear to recreate measured trends in collision frequency in our experiment. In contrast, the new closure we have derived affords a significantly higher degree of fidelity. These findings impact both the basic understanding of how IAT relates to the plume

mode physics as well as how we practically model this phenomenon. We discuss these implications in the following sections.

5.1. Influence of assumptions on results

Here we discuss how the assumptions in our analysis may be influencing our result. First, we discuss the use of a constant ion temperature in evaluating the closure models, followed by the saturated assumption that we use in our single-equation model for the IAT average frequency.

In low-temperature plasmas used in propulsion applications it is common to assume that the time average temperatures follow $\langle T_e \rangle / \langle T_i \rangle \sim 10$ [32]. We have adopted a similar assumption in this work since we were unable to measure the ion temperature with our experimental setup. Classically, the ions tend to remain cold in these systems as the heating rate through Coulomb collisions (which are infrequent in the plume region) with hot electrons is low. We therefore do not expect the ion temperature to vary greatly in the classical limit. It has been noted, however, that IAT causes ion heating that could lead to deviations from this relationship [37]. Given the large variations in IAT wave energy density we observe in our plasma, we might expect that the ion temperature could also vary accordingly. This simplifying assumption of constant T_i could therefore impact our calculation of the Sagdeev closure model (see (3)) to potentially find better agreement with the measurement.

Next, we comment on the assumption of IAT saturation that we use in our single-equation model for the average IAT frequency. This approximation implies that the energy density of IAT modes has grown sufficiently large that nonlinear interactions occur to balance with the linear growth of the waves. A common threshold for IAT, beyond which these effects become important, can be determined by examining a critical value for the static electric field induced by the effective drag due to the IAT. This expression was derived by Sagdeev [38] in the limit that nonlinear ion Landau damping balances the linear growth of the waves. The resulting critical value for the steady state electric field is given by $E_{\text{crit}} \sim 0.01 \cdot (m_e m_i^3)^{1/4} \omega_{\text{pi}} c_s / q$. The measured steady state electric field under our experimental conditions (see part I) is $E \sim 5E_{\text{crit}}$, indicating that nonlinear effects likely play a critical role in the cathode plume. Given that the plasma under investigation in this study meets this criterion, the use of the saturated limit in our model is consistent with these theoretical expectations.

5.2. Physical interpretation of the frequency-based single-equation closure model

The relative success of our model for IAT driven collision frequency suggests that this approach captures relevant physical phenomena not present in the other closures. Indeed, when experimental data is used to evaluate the single-equation closure models for the IAT wave energy density, we found that this energy quickly saturates. This in turn indicates that the saturated assumption in the zero-equation closures is approximately correct. The failure of these zero-equation models to capture the collision frequency oscillation in time, however,

points to the possibility that assuming $\langle \omega \rangle$ scales with the ion plasma frequency is overly simplistic. This may not be surprising because in order to maintain saturation, there must be some nonlinear process that prevents the energy from continuing to grow. Returning to (11), we see that the average frequency of the spectrum can be interpreted as an effective rate at which the growth of the IAT extracts energy from the electrons (thus leading to drag). Therefore we would expect that this average frequency should change to moderate the growth of the energy. The equation we derived in (13) is an attempt to capture this effect self-consistently. Physically, by employing (13) we are assuming that even if the total energy in the spectrum is saturated at the thermal limit, there will be a distribution in frequency (or equivalently lengthscale) such that growth, damping, and convection all balance to maintain the energy at this the thermal cap. This in turn translates to moderation in the rate at which the IAT extracts energy from the electrons, thereby influencing the transport.

5.3. Comparison of the expected and measured value of α

Our implementation of the frequency-based single equation closure uses an empirical scaling factor, α, that we determined by comparing the results of the model with the experimental data to find the best agreement. However, the model we have derived provides an expression for this parameter that depends on the ion Mach number, which in principle is calculated in a fluid cathode plume model (although not experimentally accessible with the methods we employed). By leveraging earlier experimental work in similarly configured cathodes we can compare our experimentally derived value to the theory.

Previous measurements using laser induced fluorescence to measure the ion velocity distribution function [27, 37, 39] in similar cathode configurations indicate that the ion drift velocity is between 4 and 6 km s^{-1}. Combined with our measured time-averaged electron temperature of 4.5 eV at $z = 0.5$ cm (see part I) we estimate the ion Mach number to be ~ 2.2–3.3. This implies that $\alpha \sim 3.2$–4.3.

The calculated scaling factor depends on the measured collision frequency and the result of the model. There is therefore an inherent uncertainty to our calculation of this parameter derived from the statistical error in the above quantities. Propagating the measurement uncertainty through, we find that $\alpha = 8.9 \pm 6$. A comparison of the theoretical and experimental results shows that although the predicted α is lower than the measurement by a factor of ~ 2–3, the expected value is within our experimental uncertainty. This favorable comparison suggests that the model for the anomalous electron collision frequency could in principle be employed in a numerical model without a tuning factor based on experimental measurements or needing to be iteratively solved for—a highly desirable feature for predictive modeling of these systems.

5.4. Comparison between measured IAT collision frequency and predictions from frequency-based, single equation closure model

Figure 3 shows that the prediction from the frequency-based single-equation closure model (figure 3(h)) actually yields

improved agreement with the measured electron collision frequency (figure 3(a)) than the measured contribution to the collision frequency from IAT (figure 3(b)). This is an unexpected result, as in principle, the closure model relies on several simplifications, whereas the IAT calculation is based on direct measurements of the IAT spectrum in the plasma (part I). There are at least two possible explanations for this relative success of the simple model. First, this closure contains the parameter, α, that that we could not determine with our measurements and that we have adjusted to yield the best agreement with the measured ν_e. Second, we have already remarked (section 4), that in the region upstream of $z < 0.3$ cm, we suspect that the presence of the probes may interfere with the propagation of the IAT. In support of this explanation, we see that the measured contribution to collision frequency from IAT drops in amplitude precipitously (pointing to the possibility of probe interference). On the other hand, the closure model only requires measurements of the background plasma properties. Since these measurements presumably are less perturbed by the presence of the probes (as they are not comprised of small-scale propagating structures), the closure model may actually better reflect the influence of the IAT in the near-field region than the wave measurements. This can in part explain the relative success of the closure in the upstream region.

With that said, we note that the prediction from the closure model does depart from the measured ν_e in some locations. In the downstream region in the particular (most clearly seen from figure 2(h)), the closure model exhibits two peaks in time for every one in the measured ν_e. This may be a consequence of the simplification we employed in the derivation of the closure and may ultimately be addressed with higher fidelity approaches. We discuss this possibility in the next section.

5.5. Methods for improving fidelity of closure models

Although the frequency-based single-equation model we have derived appears to match the measured collision frequency well, the fidelity of this closure is inherently limited. It relies on the over-restrictive assumption that the wave energy density is saturated. In practice, we might expect that the evolution of the wave energy density requires a more nuanced approach. To this point, we show in figure 4, the ratio of the measured wave energy density (inferred from the IAT spectra reported in part I) to the local thermal density, i.e. $W/n_e T_e$. If indeed the wave energy density were saturated at all times, this ratio should be constant everywhere. However, we find in figure 4 that this is not the case. This is a notable result because even though the measured wave energy deviates from our assumed saturated limit, the predicted collision frequency from the closure (the product of the IAT energy and the average collision frequency) is markedly close to ν_e. This would suggest that the oscillations in average frequency dominate, or at least compensate, for these deviations from the wave energy density from saturation in such a way as to yield an accurate model predictions (per the discussion in section 5.2). Supporting this interpretation, is the fact that the deviations in the model from the measurement are greatest in the troughs of the oscillation—the phases at which the assumption of saturated energy density
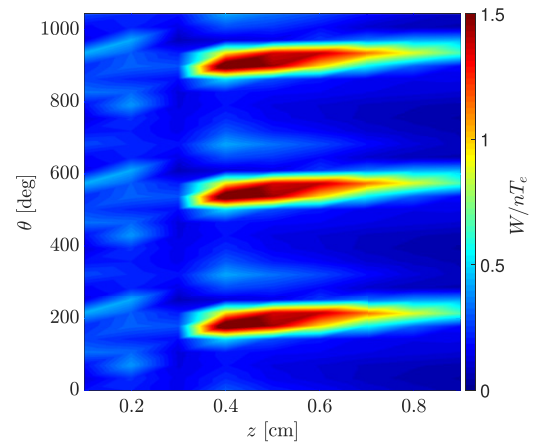
Figure 4. The ratio of the measured IAT wave energy density to the thermal energy density.

is least likely to be met. With that said, although practically our closure does yield good agreement with ν_e, figure 4 does underscore the fact that the highest fidelity approach would model both average properties of the IAT self-consistently.

In light of this limitation, the next level of complexity for turbulence modeling in cathodes would be a two-equation closure for the IAT. This method would take the form of two PDEs, one for the IAT average frequency and the other for the IAT wave energy density, allowing us to track the evolution of both parameters in space and time. Although many simplifications and assumptions are typically employed in arriving at fluid-like expressions for these parameters, these methods are beginning to show promising results when they are implemented in systems such as Hall thrusters, where an anomalous collisional phenomenon similarly dominates the transport of electrons [40].

5.6. Implications for numerical models

As we discussed in section 1 and in part I of this series, the electron motion in the hollow cathode plume is non-classical, driven by wave-related effects. In order to represent both the average and time-resolved behavior of these systems in a fluid-based numerical model, it is therefore necessary to derive closure models. While multiple models have been proposed, our work provides the first systematic experimental evaluation of these different approaches in space and time. Notably, we have shown that for our cathode, no closure models employed to date in numerical simulations (zero-equation approximations as well as single-equation approaches that follow the wave energy density) capture the time and spatial dependence of the measured ν_e.

This result has possible implications for future modeling efforts. Indeed, one of the pressing numerical challenges of cathode modeling is capturing the transition to plume mode. Given that this mode is inextricably linked to the non-classical transport (part I), in order to predict this transition and the features of the oscillations, it is critical to use the highest fidelity closure model. This raises the possibility that numerical models that rely on experimentally non-validated closures for the collision frequency may have spurious results as in

the reference [24]. With that said, we make the caveat that our conclusions about the applicability of each closure model may not be universally applicable to other studies. Previous numerical simulations [22, 23, 41] have focused on different geometries where the plasma conditions were different than those reported here. The other closures that have been proposed to date therefore may be more applicable in these alternative geometries and magnetic field configurations, which may explain their relative success in qualitatively re-creating transient behavior. In either case, the next recommendation for higher fidelity modeling is to adopt the closure we have derived here and observe the ability of the code to self-consistently capture both time-averaged and time-resolved behavior. Pending future efforts that may yield even higher fidelity models such as two-equation closures (see previous section), the model we have developed in this work is the preferable existing closure model. Further developing these types of higher-order closures for modeling IAT in cathodes could play an important role in increasing the fidelity of these models, reducing risk in space propulsion applications, and improving our understanding of transient phenomena driven by the presence of plasma turbulence in low-temperature plasma systems.

As a final comment, leaving aside full numerical solutions, identifying the right closure is equally critical for developing both a physical intuition as well as first-principles scaling laws for the onset of plume mode oscillations in cathodes. Indeed, a number of theories have been proposed to date for the mechanisms governing these oscillations [14, 20–22, 24]. Several of these theories are predicated on the existence of some feedback mechanism that exists between the plasma properties and the growth of the IAT. Understanding how the IAT depends on the background properties thus functionally is a critical requirement for identifying which processes and operating conditions facilitate the onset of this mode. The closure we have derived here offers a critical governing equation to guide future stability analysis of the cathode plume.

6. Conclusion

In summary, the goal of this two-part series has been to investigate the connection of IAT-driven transport to the large-scale oscillation exhibited by a hollow cathode in plume mode. Our earlier results in part I showed that the electron dynamics in a hollow cathode operating in plume mode are indeed non-classical with a collision frequency that exceeds the classical value by several orders of magnitude—agreeing with previous analyses of this system [15, 25, 26]. We in turn showed that this collision frequency varies on the time-scale of the plume mode oscillations ($\sim 40\,\text{kHz}$) and that this non-classical effect largely can be attributed to the presence of IAT. The goal of this second part has been to leverage the results from part I to evaluate simplified fluid-based models (closures) for the non-classical electron collision frequency. This was motivated by the fact that most state-of-the-art models for hollow cathode simulations are fluid-based and therefore cannot self-consistently model the effects of IAT. Moreover, it recently has come to light from numerical simulations, that the dynamical behavior of the effective collision frequency must

be modeled in some way in order to re-create the transition to plume mode.

In this work, we have considered all of the existing closure models for the non-classical collision frequency that have been employed to date and derived a new one. We classified the closures based on complexity with zero-equation models relying on algebraic expressions for the collision frequency while single-equation models required a solution of a single, one-dimensional PDE. We then evaluated these models by using experimental measurements of the background plasma properties and then compared their predictions to the measured collision frequency. We ultimately found that although some of the closure models we investigated—both zero-equation and single-equation—have been successfully used to capture the time-average trends of the cathode plume, they do not yield time-resolved predictions consistent with our experimental measurements of the collision frequency. On the other hand, the new closure we derived based on a single-equation model that tracks the evolution of the average frequency of the IAT spectrum, yielded excellent quantitative agreement with the measured electron collision frequency over the 1D experimental domain.

We have discussed the physical significance of this result in the context of the properties of the IAT. In particular, our result physically supports the interpretation that the IAT remains approximately saturated in the cathode plume, and the rate at which the IAT draws energy from the electrons (the effective collision frequency) self-consistently adjusts to maintain this saturated state. This procedure inherently accounts for the non-linear behavior that occurs during the saturation of the waves, a process that is not captured in any other model that has been employed to date. We also discussed that the fidelity of future numerical models will be improved by adopting this validated experimental closure. Though, there are limitations to this physical interpretation—a closer inspection of the measured wave energy density reveals that it is not in fact saturated at all times. We have discussed potential future directions to capture this phenomenon including adopting a more sophisticated two-equation closure. Ultimately, this study and the relative success of our novel closure model ultimately lays the foundation for new physical understanding of the dynamics of the hollow cathode discharge undergoing plume mode oscillations and for accurately capturing these effects with numerical modeling.

ORCID iDs

Marcel P Georgin ⬤ https://orcid.org/0000-0003-3733-1682
Benjamin A Jorns ⬤ https://orcid.org/0000-0001-9296-2044

References

[1] Pots B F M 1979 Turbulence and Transport in a Magnetized Argon Plasma *PhD Thesis* Eindhoven Tech. University
[2] Pots B F M, Coumans J J H and Schram D C 1981 *Phys. Fluids* **24** 517–27
[3] Ngo M T, Schoenbach K H, Gerdin G A and Lee J H 1990 *IEEE Trans. Plasma Sci.* **18** 669–76
[4] Arbel D, Bar-Lev Z, Felsteiner J, Rosenberg A and Slutsker Y Z 1993 *Phys. Rev. Lett.* **71** 2919–22
[5] He S J, OuYang J T, Shang L and Feng H 2011 *IEEE Trans. Plasma Sci.* **39** 2514–5
[6] Harrison W W and Magee C W 1974 *Anal. Chem.* **46** 461–4
[7] Muhl S and Pérez A 2015 *Thin Solid Films* **579** 174–98
[8] Goebel D M and Chu E 2014 *J. Propul. Power* **30** 35–40
[9] Paschen F and Heliumlinien B 1916 *Ann. Phys.* **355** 901–40
[10] Goebel D M and Watkins R M 2010 *Rev. Sci. Instrum.* **81** 083504
[11] Csiky G A 1969 Measurements of Some Properties of a Discharge from a Hollow Cathode *Technical Note* NASA
[12] Philip C M 1971 *AIAA J.* **9** 2191–6
[13] Friedly V J and Wilbur P J 1992 *J. Propul. Power* **8** 635–43
[14] Goebel D M, Jameson K K, Katz I and Mikellides I G 2007 *Phys. Plasmas* **14** 103508 (1994-present)
[15] Mikellides I G, Katz I, Goebel D M, Jameson K K and Polk J E 2008 *J. Propul. Power* **24** 866–79
[16] Kerslake W R and Rawlin V K 1970 *J. Spacecr. Rockets* **7** 14–20
[17] Pedrini D, Albertoni R, Paganucci F and Andrenucci M 2015 *Acta Astronaut.* **106** 170–8
[18] Potrivitu G-C, Joussot R and Mazouffre S 2018 *Vacuum* **151** 122–32
[19] Georgin M P, Jorns B A and Gallimore A D 2019 *Phys. Plasmas* **26** 082308
[20] Csiky G A 1969 Investigation of a Hollow Cathode Discharge Plasma *AIAA Electric Propulsion Conf.*
[21] Mandell M and Katz I 1994 Theory of Hollow Operation in Spot and Plume Modes *30th Joint Propulsion Conf.*
[22] Mikellides I, Lopez Ortega A, Goebel D M and Becatti G 2020 *Plasma Sources Sci. Technol.* **29** 035003

[23] Sary G, Garrigues L and Boeuf J-P 2017 *Plasma Sources Sci. Technol.* **26** 055007
[24] Sary G, Garrigues L and Boeuf J-P 2017 *Plasma Sources Sci. Technol.* **26** 055008
[25] Mikellides I G, Katz I, Goebel D M and Jameson K K 2007 *J. Appl. Phys.* **101** 063301
[26] Jorns B A, Mikellides I G and Goebel D M 2014 *Phys. Rev.* E **90** 063106
[27] Jorns B A, Dodson C, Goebel D M and Wirz R 2017 *Phys. Rev.* E **96** 023208
[28] Lopez Ortega A, Jorns B A and Mikellides I G 2018 *J. Propul. Power* **34** 1026–38
[29] Georgin M P, Jorns B A and Gallimore A D 2020 *Plasma Sources Sci. Technol.* **29** 105010
[30] Sagdeev R Z and Galeev A A 1969 *Nonlinear Plasma Theory* (New York: W.A Benjamin)
[31] Tsytovich V N 1995 *Lectures on Non-linear Plasma Kinetics* (Berlin: Springer)
[32] Goebel D M and Katz I 2008 *Fundamentals of Electric Propulsion: Ion and Hall Thrusters* vol 1 (New York: Wiley)
[33] Davidson R C and Krall N A 1977 *Nucl. Fusion* **17** 1313
[34] Stix T H 1962 *The Theory of Plasma Waves* (New York: McGraw-Hill)
[35] Lafleur T, Baalrud S D and Chabert P 2016 *Phys. Plasmas* **23** 053503
[36] Huba J D 2016 *NRL Plasma Formulary* (Washington DC: US Naval Research Laboratory)
[37] Dodson C A, Perez-Grande D, Jorns B A, Goebel D M and Wirz R E 2018 *J. Propul. Power* **34** 1225–34
[38] Sagdeev R Z 1979 *Rev. Mod. Phys.* **51** 1–9
[39] Williams G J Jr, Smith T B, Domonkos M T, Gallimore A D and Drake R P 2000 *IEEE Trans. Plasma Sci.* **28** 1664–75
[40] Jorns B A 2019 Two equation closure model for plasma turbulence in a Hall effect thruster *36th Int. Electric Propulsion Conf. (IEPC)* vol 129 (Vienna, Austria) (Electric Rocket Propulsion Society)
[41] Lopez Ortega A, Mikellides I G, Sekerak M J and Jorns B A 2019 *J. Appl. Phys.* **125** 033302